Biophysical Chemistry 167 (2012) 26–35

Contents lists available at SciVerse ScienceDirect

Biophysical Chemistry

journal homepage: http://www.elsevier.com/locate/biophyschem

Comparative biophysical characterization of chicken β_2-microglobulin

Chee-Seng Hee [a], Heinz Fabian [b], Barbara Uchanska-Ziegler [a], Andreas Ziegler [a,*], Bernhard Loll [c,**]

[a] Institut für Immungenetik, Charité - Universitätsmedizin Berlin, Campus Benjamin Franklin, Freie Universität Berlin, Thielallee 73, 14195 Berlin, Germany
[b] Robert Koch Institut, ZBS 6, Nordufer 20, 13353 Berlin, Germany
[c] Institut für Chemie und Biochemie, Abteilung Strukturbiochemie, Freie Universität Berlin, Takustrasse 6, 14195 Berlin, Germany

HIGHLIGHTS

- Investigation of 3 chicken subtypes, BF2*2101, BF2*1301 and YF1*7.1 and free β_2m.
- The structure of free chicken β_2m was determined to 2.0 Å resolution.
- DSC indicated that chicken molecules are stabilized in an allele-dependent fashion.
- H/D exchange behavior of chicken/human β_2m was studied by infrared spectroscopy.
- Chicken β_2m shows an increased conformational flexibility

GRAPHICAL ABSTRACT

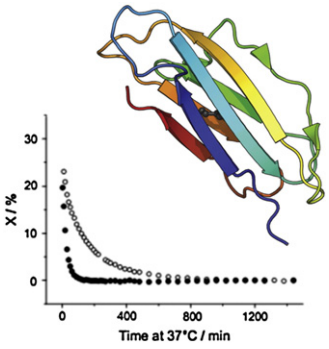

ARTICLE INFO

Article history:
Received 20 February 2012
Received in revised form 2 April 2012
Accepted 5 April 2012
Available online 14 April 2012

Keywords:
X-ray crystallography
β_2-microglobulin
Immune system
Major histocompatibility complex
IR spectroscopy
Differential scanning calorimetry

ABSTRACT

β_2-microglobulin (β_2m) is the smallest building block of molecules belonging to the immunoglobulin superfamily. By comparing thermodynamic and structural characteristics of chicken β_2m with those of other species, we seek to elucidate whether it is possible to pinpoint features that set the avian protein apart from other β_2m. The thermodynamic assays revealed that chicken β_2m exhibits a lower melting temperature than human β_2m, and the H/D exchange behavior observed by infrared spectroscopy indicates a more flexible structure of the former protein. To understand these differences at a molecular level, we determined the structure of free chicken β_2m by X-ray crystallography to a resolution of 2.0 Å. Our comparisons indicate that certain biophysical characteristics of the chicken protein, particularly its conformational flexibility, diverge considerably from those of the other β_2m analyzed, although basic structural features have been retained through evolution.

1. Introduction

β_2-microglobulin (β_2m) is a protein composed of 99 residues which folds into a seven-stranded β-sandwich fold [1]. The strands are termed A to G and the loops are designated according to the strands which they connect, e.g. AB, BC, CD, and so on. The typical immunoglobulin fold of β_2m comprises two β-sheets (strands A, B, D, E on one hand and strands C, F, G on the other) mediated by a highly conserved intra-molecular S–S bridge with a spacing of ~54 amino acids between the two cysteine residues of the protein. Structurally, β_2m constitutes the basic building unit of the immunoglobulin superfamily[2]. In addition, the protein serves as a light chain that is non-covalently bound to the heavy chain (HC) of major histocompatibility complex (MHC) class I or class I-like molecules such as CD1 [3,4].

The presence of β_2m is an important prerequisite for the binding of small ligands by MHC class I molecules [5]. Although such ligands

* Corresponding author. Tel.: +49 30 450 564731; fax: +49 30 450 564920.
** Corresponding author. Tel.: +49 30 838 57348; fax: +49 30 450 838 54936.
E-mail addresses: andreas.ziegler@charite.de (A. Ziegler), loll@chemie.fu-berlin.de (B. Loll).

0301-4622/$ – see front matter © 2012 Elsevier B.V. All rights reserved.
doi:10.1016/j.bpc.2012.04.001

are anchored within a groove that is formed by the HC, β_2m is crucial for maintaining complex stability as well [6,7], and for the intracellular transport of the complex to the surface of nearly all nucleated cells [8–11]. Free β_2m, on the other hand, is found in most body fluids [12] including serum, urine, milk and colostrum [13–15]. In humans, the protein is normally eliminated by the kidney, but it forms deposits as amyloid fibrils within joints as a consequence of long-term hemodialysis treatment of patients, known as dialysis-related amyloidosis [16,17]. Forms of amyloidosis have been described in chickens [18], but there are no reports that β_2m deposition is the cause.

Although chicken and human β_2m share only ~48% amino acid sequence similarity, both molecules may serve as the light chain in MHC class I molecules. While analyzing the avian lipid-binding MHC class I molecule YF1*7.1, our previous calorimetric measurements revealed that chicken β_2m in this complex is less thermostable than its human counterpart [19]. To gain further insight into the thermodynamic properties of chicken β_2m and its conformational flexibility, we studied this molecule by differential scanning calorimetry (DSC) and infrared (IR) spectroscopy. In addition, as structural information was limited to complexes of this molecule with divers HC, i.e. the peptide-binding BF2*2101, [20], YF1*7.1 [19], and CD1-1 [21], we additionally determined the crystal structure of free chicken β_2m by X-ray crystallography. The results allow us not only to compare free β_2m from two mammalian, an avian, and a fish species, but also permit us to suggest structure-based explanations for a number of biophysical properties of these proteins.

2. Methods

2.1. β_2m purification

The coding sequence for the extra-cellular domain of β_2m (residues 21–120 of the signal peptide-containing protein) was cloned into the expression vector pMAL-p4x, expressed as maltose-binding protein fusion construct (MBP-β_2m) and purified using the pMAL purification system (New England Biolabs, Frankfurt, Germany). *Escherichia coli* TB1 cells transformed with the MBP-β_2m construct were grown at 310 K in LB-medium containing 100 mg/l ampicillin to an OD_{600} of 0.5. Protein expression was induced by adding 0.4 mM isopropyl β-D-1-thiogalactopyranoside and cells were incubated for 20 h at 298 K and then harvested by centrifugation at 4500 g for 10 min at 277 K. The MBP-β_2m fusion protein was extracted from the periplasm according to the pMAL purification protocol. The cell pellet obtained by centrifugation was resuspended and incubated in 100 ml buffer containing 30 mM Tris–HCl pH 8.0, 20% (w/v) sucrose, 1 mM EDTA and 0.3 mM phenylmethanesulfonylfluoride (PMSF) on a shaker for 10 min. After incubation, the sample was centrifuged at 8000 *g* for 10 min at 277 K and the pellet was resuspended in 100 ml chilled 5 mM $MgSO_4$ followed by incubation for 10 min in an ice bath. The sample was then centrifuged at 8000 g for 10 min at 277 K; the supernatant was collected and filtered through a 0.22 μm filter membrane (Millipore, Schwalbach, Germany). The filtered sample was applied onto a 10 ml self-packed amylose resin (New England Biolabs, Frankfurt, Germany) column, washed with 100 ml column buffer (20 mM Tris–HCl pH 7.5, 200 mM NaCl, 1 mM EDTA) and eluted with 30 ml column buffer containing 10 mM maltose. Fractions containing the MBP-β_2m fusion protein were collected and concentrated using an Amicon Ultra-15 protein centrifugal filter with 10 kDa molecular weight cutoff (Millipore) before purification by size exclusion chromatography on a Superdex™ 200 16/60 column (GE Healthcare, Freiburg, Germany) connected to an ÄKTA FPLC instrument (GE Healthcare, Germany). The MBP-tag was cleaved with protease factor Xa (New England Biolabs, Frankfurt, Germany) by incubation at 296 K for 2 days. β_2m was separated from MBP using a 10 ml self-packed amylose resin column followed by purification on a Superdex™75 column (GE Healthcare, Freiburg, Germany) in a buffer composed of 20 mM Tris–HCl pH 7.5, 150 mM NaCl, and 0.01% (w/v) sodium azide. The purity of the protein was assessed by SDS-PAGE. The protein concentration was determined by measuring the absorption at a wavelength of 280 nm, assuming an absorption coefficient of 19200 M^{-1} cm^{-1}. Human β_2m was prepared as previously described [22].

2.2. Preparation of YF1*7.1, BF2*1301:pMDV and BF2*2101:pC1 complexes

The cDNA sequences of the extracellular domains of BF2*1301 and BF2*2101 (residues 22–294) were cloned into the pMAL-p4x vector. Both clones were verified by DNA sequencing. Preparation and purification of chicken β_2m and the YF1*7.1 complex have been reported previously [23]. For the BF2*1301 and BF2*2101 complexes, a similar protocol was established with slight modifications. The MBP-fused BF2*1301 and BF2*2101 HC were expressed as inclusion bodies in *E. coli* TB1 cells. The HC were refolded in a reconstitution buffer together with solubilized β_2m and a peptide. For the reconstitution of BF2*1301, the pMDV peptide (^{153}VDAYDRDE^{160}) derived from *Meleagrid herpesvirus* glycoprotein B was used, whereas the pC1 peptide (^{353}SELKDFFQKL^{362}) is derived from *Gallus gallus* Ras-GTPase-activating protein and was employed for reconstitution of BF2*2101 [24]. Both peptides were purchased from Alta Bioscience, UK. Refolding was performed according to the established protocol for HLA class I complexes [22,25]. Reconstituted protein complexes were subjected to Factor Xa digestion to remove the MBP-tags, followed by an affinity chromatography step on an amylose column and gel filtration chromatography as described [23].

2.3. Differential scanning calorimetry

Excess heat capacity curves were recorded using an ultrasensitive scanning micro-calorimeter (VP-DSC, MicroCal Inc., Northampton, MA, USA) with a heating rate of 1 K/min and a sample cell volume of 0.5 ml. For refolding experiments, after the initial heating from 20 °C to 90 °C, the samples were cooled to 20 °C and subsequently heated again to 90 °C. All DSC samples were prepared in 10 mM phosphate buffer (pH 7.5), 150 mM NaCl and the protein concentrations were adjusted to the range of 0.18–0.22 mg/ml. DSC measurements were conducted as described previously by us for HLA–B27 complexes [25]. The experimental data were analyzed by standard procedures using the "ORIGIN for DSC" software package supplied by the manufacturer.

2.4. Infrared spectroscopy

The protein solutions were always freshly prepared and placed into demountable calcium fluoride IR-cells with an optical pathlength of 50 μm for measurements in D_2O-buffer or 8 μm for samples in H_2O-buffer. IR-spectra were recorded with IFS-28B and IFS-66 Fourier transform infrared (FTIR) spectrometers (Bruker Optics, Ettlingen, Germany) equipped with DTGS (deuterated triglycine sulphate) detectors and continuously purged with dry air. For each sample, 128 interferograms were co-added and Fourier-transformed to yield spectra with a nominal resolution of 4 cm^{-1}. The sample temperature was controlled by means of thermostated cell jackets. Buffer spectra were recorded under identical conditions and subtracted from the spectra of the proteins in the relevant buffer (10 mM sodium phosphate, pH 7.5, 150 mM NaCl). Spectral contributions from residual water vapor, if present, were eliminated using a set of water vapor spectra. The final unsmoothed protein spectra were used for further analysis. Band intensities were determined by standard functions of the Bruker OPUS software, implemented into home-built macros for data analysis. A detailed account of the entire procedure has been given previously [26].

2.5. Crystallization and crystal cooling

β_2m with a concentration of 17 mg/ml was used for crystallization experiments. Initial crystals were obtained at 291 K in a sitting drop

setup in 96-well plates although the crystals were insufficient in size for X-ray data collection. The crystal size could be improved in a hanging drop setup using a reservoir solution with a volume of 700 µl composed of 22% (w/v) polyethylene glycol 3350 and 200 mM $MgCl_2$ at a final pH of 5.6. The crystallization drop was mixed from 1.5 µl chicken β_2m and 1.5 µl reservoir solution. Needle-shaped, inter-grown crystals appeared after 3 weeks. Inter-grown needles were carefully separated with an acupuncture needle yielding single thin specimens. Prior to cooling, the crystals were transferred to a cryo-solution containing 25% (w/v) polyethylene glycol 3350, 200 mM $MgCl_2$, and 20% (v/v) glycerol. They were subsequently flash cooled in liquid nitrogen.

2.6. X-ray data collection, structure determination and refinement

Synchrotron diffraction data were collected at the beamline 14.2 of the MX Joint Berlin laboratory at the BESSY in Berlin, Germany. X-ray data collection was performed at 100 K at a wavelength of $\lambda = 0.9184$ Å and diffraction data were processed with the XDS package [27]. For calculation of the free R-factor, a randomly generated set of 5% of the reflections from the diffraction data set was used and excluded from the refinement. Initial phases were determined by molecular replacement with the program PHASER [28] employing the coordinates of β_2m from the structure of BF2*2101 (PDB entry: 3BEW) [20]. The structure was refined by maximum-likelihood restrained refinement implemented in REFMAC5 [29] followed by iterative model building cycles with COOT [30]. Water molecules were picked with COOT [30] and manually inspected. At final stages of refinement, TLS refinement [31] was applied with one TLS-group for each polypeptide chain. Model quality was evaluated with PROCHECK [32] and MolProbity [33]. Secondary structure elements were assigned with DSSP [34]. Superposition of structures was performed with SUPERPOSE Secondary-Structure Matching (SSM) [35], as implemented in the CCP4 package. Structures were analyzed for internal cavities with the program CASTp [36] and visually examined in PyMOL [37]. Shape complementarity analysis was performed with the program SC

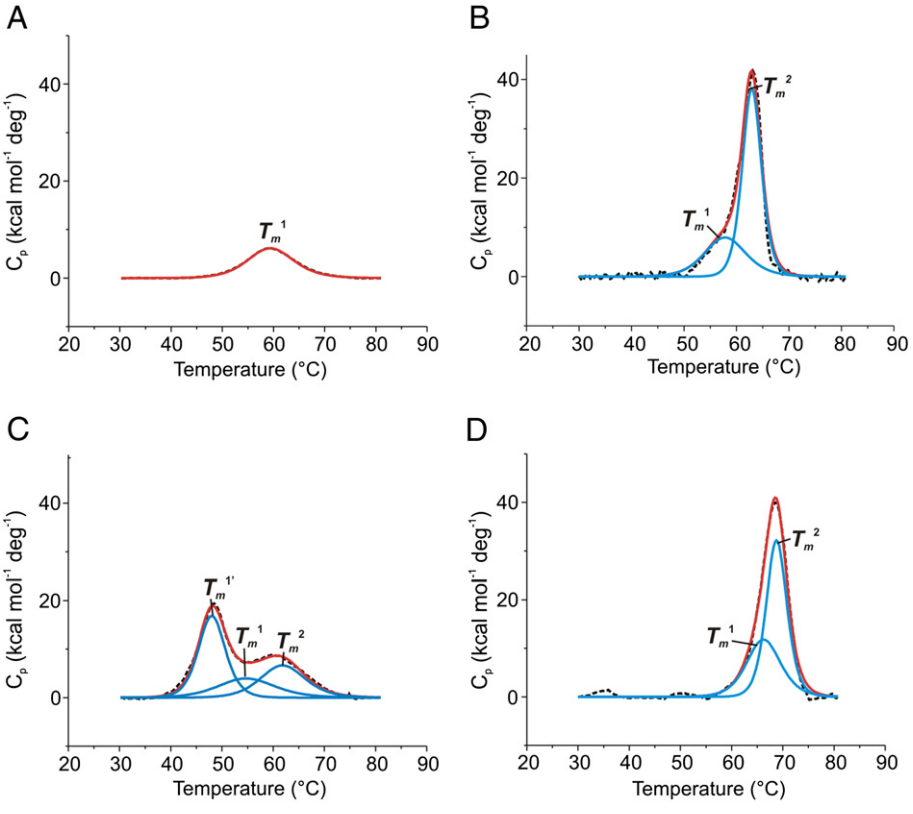

E

Sample	*n*	$T_m^{1'}$	$\Delta H_m^{1'}$	T_m^{1}	ΔH_m^{1}	T_m^{2}	ΔH_m^{2}	ΔH_m^{tot}
β_2m	6			59.1 ± 0.3	73.5 ± 2.0			73.5
BF2*2101:pC1	2			57.8 ± 0.1	80.9 ± 3.1	63.0 ± 0.1	183.8 ± 1.9	264.7
YF1*7.1	4	47.7 ± 1.0	117.5 ± 6.4	57.9 ± 1.8	76.3 ± 10.5	64.1 ± 2.1	74.7 ± 2.3	268.5
BF2*1301:pMDV	2			66.2 ± 0.1	98.7 ± 7.5	68.6 ± 0.3	175.7 ± 4	274.4

n is number of measurements; T_m is in °C; ΔH is in kcal^{-1}

Fig. 1. Stabilities of β_2m and MHC class I complexes of the chicken. The thermodynamic stabilities were determined by differential scanning calorimetry (DSC). Experimental excess heat capacity curves (black dashed lines) and deconvolution curves (blue lines) as well as the calculated fit (red lines) obtained from DSC of (A) free β_2m, (B) BF2*2101:pC1 complex, (C) YF1*7.1 complex, and (D) BF2*13:pMDV complex. (E) The table summarizes the deconvoluted melting temperatures (T_m) and enthalpy changes (ΔH_m) from DSC experiments. ΔH_m^{tot} is the total enthalpy change that accompanies a given melting process.

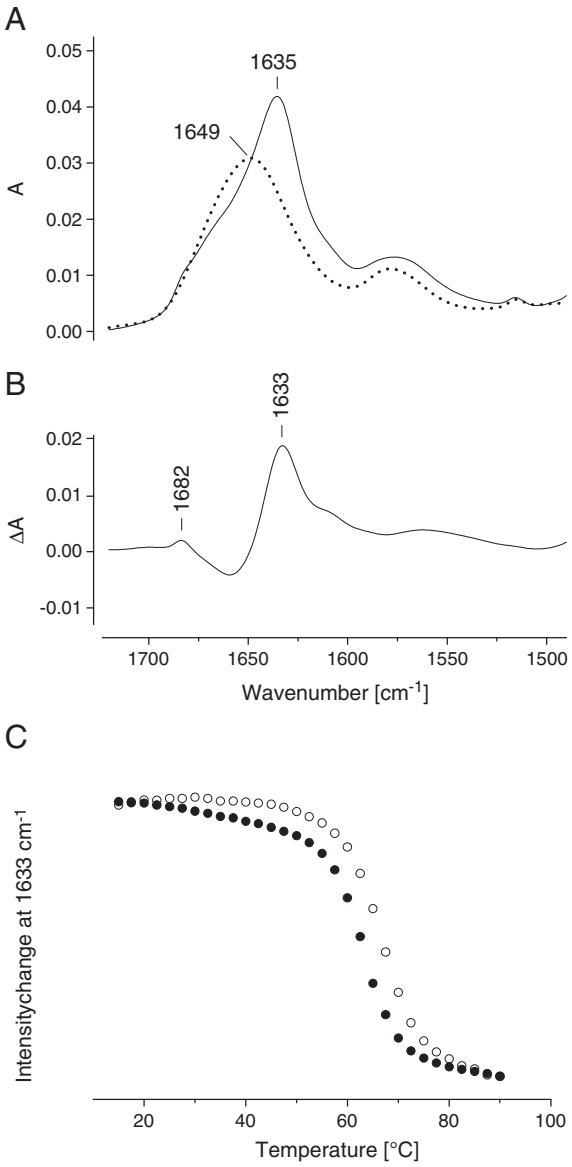

Fig. 2. Thermostabilities of free chicken β_2m and free human β_2m monitored by IR spectroscopy. (A) IR spectra of chicken β_2m after complete H/D exchange at 15 °C (continuous line) and at 90 °C (dotted line). (B) IR difference spectrum obtained upon subtracting the spectrum of unfolded chicken β_2m at 90 °C from that of the folded protein at 15 °C, illustrating the spectral changes associated with the unfolding the β-sheet structure of chicken β_2m. (C) Unfolding of chicken β_2m (filled circles) and human β_2m (open circles) at protein concentrations of ~1 mg/ml monitored by the temperature-induced changes in absorbance at 1633 cm^{-1}. Exchange of all amide protons with deuterons in human β_2m was achieved by keeping the protein solution overnight at 37 °C. Details and IR band assignments are described in [26].

[38] implemented in the CCP4 package. Figures were prepared using PyMOL [37] and 3D figures were produced as described previously [39]. The 3D figure can be activated by clicking on the image. Each model (structure) can be selected or removed by checking the boxes in the model tree, which is available upon clicking on the icon to the right of the "Views" drop-down menu. Preset views are shown below the model tree and can be displayed in the form of a "tour" by clicking the green arrows in the middle of the opened model tree menu. A 3D session can be terminated by right-clicking anywhere onto the model and choosing "Disable 3D". The atomic coordinates and structure factor amplitudes have been deposited in the Protein Data Bank under the accession code 3O81.

3. Results and discussion

3.1. Thermodynamic properties of chicken β_2m and MHC class I complexes

The presence of β_2m has been described as a prerequisite for the stabilization of mammalian MHC class I complexes [6,7]. While the same was suspected for avian MHC class I molecules, systematic studies of these proteins had not been carried out so far. Our reconstitution experiments with three different classical chicken subtypes, BF2*2101, BF2*1301 and YF1*7.1 together with β_2m clearly revealed

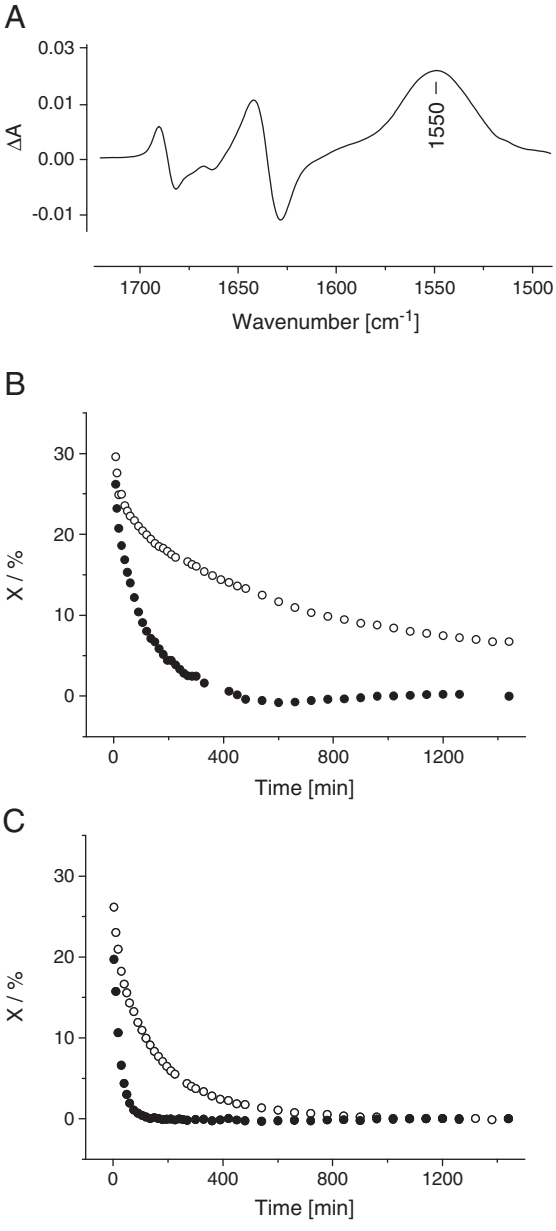

Fig. 3. H/D exchange behavior of free chicken β_2m and free human β_2m at protein concentrations of ~5 mg/ml. (A) IR difference spectrum obtained upon subtracting the spectrum of chicken β_2m kept at 25 °C for 24 h in D_2O-buffer from that of chicken β_2m 7 min after dissolution in D_2O-buffer. Loss of residual unexchanged amide groups in chicken β_2m (filled circles) and human β_2m (open circles) at 25 °C (B) and 37 °C (C) as monitored by IR spectroscopy. X is the fraction of the unexchanged amide protons as calculated by setting the difference in peak intensity at 1550 cm^{-1} (amide II band) between the spectra in H_2O-buffer and after 24 h in D_2O-buffer at 37 °C to 100%.

the absolute requirement of the light chain for complex reconstitution [19,23]. DSC was employed to assess, in addition to MHC class I complexes, also the thermodynamic stability of free β_2m. This protein exhibited a single two-state transition upon temperature increase, with a melting temperature (T_m) of ~59.1 °C (Fig. 1A, E), about 5 °C lower than that of human β_2m [25]. The unfolding enthalpies of the two proteins, however, were practically indistinguishable. Furthermore, the folding reversibility of chicken β_2m was found to be akin to that of human β_2m with regard to the reversibility of folding: ~70% of the unfolded protein refolded when cooled to 20 °C [25].

These results are supported by thermal unfolding experiments of chicken β_2m performed by IR spectroscopy (Fig. 2A, B), which confirm a decreased T_m value of ~4 °C for chicken β_2m when compared to human β_2m (Fig. 2C). In addition, we studied the hydrogen/deuterium (H/D) exchange behavior of the two proteins by monitoring the disappearance of the amide II band near 1550 cm^{-1} in the IR-spectra (Fig. 3A). This approach can provide valuable information on the structure and flexibility of proteins [40]. Lyophilized samples were dissolved in D_2O buffer and the time course and extent of exchange of the amide protons with deuterons in the samples, kept at 25 °C and 37 °C, respectively, were measured over a period of 24 h. The IR-data revealed that already shortly after dissolution (first data point measured 3 min after starting the experiment), 70–75% (at 25 °C) and 75–80% (at 37 °C), respectively, of the N–H groups were exchanged by deuterons in chicken as well as human β_2m (Fig. 3A, B). The degree of exchange was initially only slightly lower for human β_2m than for chicken β_2m, but these differences in H/D exchange became more pronounced over time. At room temperature, it took ~10 h to fully exchange all N–H groups of chicken β_2m, while ~10% remained unexchanged in human β_2m even after 1 day at 25 °C (Fig. 3B). As expected, an increase in temperature made the proteins more prone to H/D exchange, resulting in a faster loss of residual N-H groups in chicken than in human β_2m at 37 °C (Fig. 3C). Generally, protons exposed to the solvent and involved in unstable regions of a protein will exchange rapidly, whereas those protons that are part of the hydrophobic core of a protein are typically much more resistant to exchange.

We then analyzed whether these properties of free chicken β_2m could also be observed in the HC-complexed form by using DSC. As expected, the experimental excess heat capacity curves of chicken BF2*2101:pC1 and BF2*1301:pMDV were more complex than that of free β_2m. They could each be deconvoluted into two two-state transitions (Fig. 1B, D, E), while the YF1*7.1 complex was clearly less stable (Fig. 1C, E). Unfolding of this complex started at 40 °C, a value that is lower than the body temperature (41.8 °C) of a chicken [41] and the experimental excess heat capacity curve could be deconvoluted into three 2-state transitions with the T_m peaks at 48 °C, 58 °C and 64 °C (Fig. 1C). We have already argued that these characteristics are connected to the lack of an appropriate ligand within the binding groove of YF1*7.1 [19]. In addition to being distinct from the latter, the unfolding behaviors of the BF2 complexes were not identical either. Two-state transitions corresponding to two T_m peaks at ~58 °C and ~63 °C (Fig. 1B, E) characterize the BF2*2101:pC1 complex, whereas the BF2*1301:pMDV complex was more stable with a first T_m of ~66 °C and a second T_m at ~69 °C (Fig. 1D, E). This could be due to the unusual anchor amino acid requirement of the BF2*1301 protein, which binds only peptides with three appropriately spaced acidic residues [42]. All three chicken complexes did not refold when cooled down to 20 °C after the first heating step to 90 °C (Fig. S1), as reported previously by us for HLA–B27 complexes employing identical experimental conditions [25].

An interpretation of these distinct melting behaviors found by DSC experiments is not straightforward, although it may be aided by considering the T_m values in conjunction with the corresponding unfolding enthalpies for a given complex and a comparison with the values obtained with free β_2m. For example, the first transition (T_m1') of the YF1*7.1 complex is very likely not due to unfolding of β_2m, because the temperature is much too low and the enthalpy does not correspond to that of free β_2m (Fig. 1C, E). This transition should therefore reflect the partial melting of the HC. Whether one of the next two

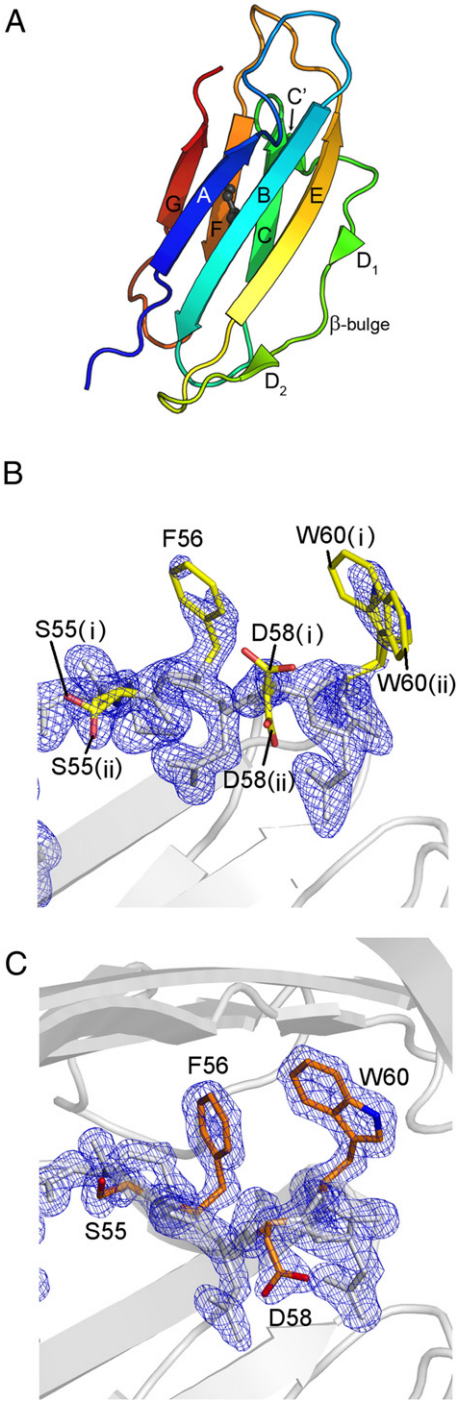

Fig. 4. Structural details of chicken β_2m. (A) Cartoon representation of chicken β_2m. The rainbow chain is colored from N-terminus (dark blue) to C-terminus (red) with the β-strands labeled from A to G. The first β-sheet is formed by β-strands A, B, D_1, D_2, and E, while the second β-sheet comprises β-strands C, F and G. The two β-sheets are connected by a disulfide bond which is shown in black as ball-and-stick representation. (B and C) The final 2*Fo-Fc* electron density maps in blue are contoured at a level of 1.5 σ. Selected residues of free β_2m with multiple conformations or poorly defined electron density are displayed as yellow stick representation (B), double conformations are indicated with (i) and (ii) following residue numbering. (C) Selected flexible residues of chicken β_2m are stabilized (orange stick representation) upon binding to YF1*7.1 HC drawn in grey as cartoon representation) (PDB entry: 3P77).

transitions (T_m1 and T_m2) is due to unfolding of β_2m, as suggested by the enthalpies observed, to further unfolding of the YF1*7.1 HC or a combination of both, is impossible to deduce from these DSC experiments. Similarly, from a comparison with the values obtained for free β_2m, it seems plausible to assume that T_m1 reflects the melting of β_2m from the BF2*2101:pC1 complex. In the case of BF2*1301:pMDV, the HC must contribute to both melting temperatures observed for the complex, but it remains unknown whether β_2m melts as part of the first or the second transition. The DSC experiments do show, however, that chicken MHC class I molecules are stabilized in an allele-dependent fashion when bound to appropriate ligands. Melting temperatures higher than that of free β_2m can thus be obtained, e.g. in the case of BF2*1301 complexes. This has also been observed in the case of selected human HLA class I complexes [25,43].

3.2. Overall structure

To obtain information on the structural basis for the observed conformational flexibility of chicken β_2m, we decided to crystallize the protein and to determine its structure. Free chicken β_2m (residues 21–120 of the signal peptide-containing protein) was purified [23] and successfully crystallized. Using synchrotron radiation, an X-ray diffraction data set was collected at 2.0 Å resolution (Table 1). The structure (Fig. 4A) was solved by molecular replacement, employing the structure of chicken β_2m in complex with BF2*2101 (protein data bank PDB entry: 3BEW) [20] as a model. Refinement of the structure converged with an R/R_{free}-factor of 19.5/24.3%. The geometry of the structure is excellent with no Ramachandran outliers. Detailed refinement statistics are given in Table 1. The electron density was of excellent quality, allowing the unambiguous tracing of the polypeptide chain, even in the case of the few residues that were found to display multiple conformations (Fig. 4B). These residues are stabilized upon binding of the molecule to an MHC class I HC (Fig. 4C). The model is complete except for the two carboxy-terminal amino acid residues.

Chicken β_2m adopts the classical fold of the immunoglobulin domain with a seven-stranded β-sandwich fold (Fig. 4A) that is composed of two β-sheets arranged face-to-face. These are connected and stabilized by a disulfide bond between Cys25 and Cys80 on β-strands B and F, respectively. The β-strand assignment is according to Saper and colleagues [3] and resembles that used for human β_2m. The first β-sheet is composed of β-strands A, comprising the residues 6–11 (A^{6-11}), B^{21-30}, D_1^{50-51} and D_2^{55-56}, as well as E^{62-70}, and the second β-sheet is formed by C^{36-41}, F^{78-83}, and G^{91-95} (Fig. 4A). Additionally, a short β-strand is located between the β-strands C and D which is termed C′. It encompasses residues 44 and 45. The β-strands D_1 and D_2 are separated by a three residue long β-bulge that is twisting the β-strand (Fig. 4A). When complexed with the HC, such an arrangement allows for efficient interaction. The crystallographic asymmetric unit harbors two chicken β_2m polypeptide chains that are practically indistinguishable with a root mean square deviation (r.m.s.d.) of 0.3 Å for 97 pairs of Cα-atoms.

Table 1
Data collection and refinement statistics.

Data collection	
PDB entry	3O81
Space group	$P2_1$
Unit cell a; b; c [Å]	36.9; 30.5; 87.4
α; β; γ [°]	90.0; 87.4: 90.0
Resolution [Å] [a]	30.0–2.0 (2.1–2.0)
Completeness [%][a]	96.0 (92.2)
$<I/\sigma(I)>$[a]	12.5 (6.8)
R_{meas}[b]	8.8 (19.3)
Redundancy[a]	3.6 (3.5)
Refinement	
Non-hydrogen atoms	1765
R_{work} [a,c]	19.5 (19.3)
R_{free}[a,d]	24.2 (22.0)
Overlay of monomeric bo_2m (chain A), no. of atoms/average B factor [Å^2]	810/18.0
Overlay of monomeric bo_2m (chain B), no. of atoms/average B factor [Å^2]	801/19.0
Water, no. of molecules/average B factor [Å^2]	160/23.8
Rmsd[e] from ideal geometry, bond length [Å]	0.011
bond angles [°]	1.271

[a] Values in parentheses refer to the highest resolution shell.
[b] $R_{meas} = \Sigma_h\,[n/(n-1)]^{1/2}\ \Sigma_i|I_h - I_{h,i}|/\ \Sigma_h\Sigma_i\ I_{h,i}$.where I_h is the mean intensity of symmetry-equivalent reflections and n is the redundancy.
[c] $R_{work} = \Sigma_h\,|F_o - F_c|\,/\,\Sigma\,F_o$ (working set, no σ cut-off applied).
[d] R_{free} is the same as R_{cryst}, but calculated on 5% of the data excluded from refinement.
[e] Root-mean-square deviation (Rmsd) from target geometries.

3.3. Monomer–monomer interface

The monomer–monomer interface within the asymmetric unit is exclusively hydrophobic, leading to a head-to-head arrangement of the loop connecting strands B and C (BC loop) and the D_2E loop of both β_2m molecules (Fig. 5A, B). Further analyses revealed additional crystal contacts between adjacent symmetry-related molecules due to tight packing. The solvent content of the chicken β_2m crystal (34.5%) is significantly lower than that of human (44.2%), bovine (55.0%) and carp (51.1%). The hydrophobic interactions between the two chicken β_2m molecules appear so far to be unique, since such an interface has not been observed in other structures of free β_2m. By formation of this hydrophobic interface *in crystallo*, a number of hydrophobic amino acid residues (Fig. 5B) are shielded from the solvent, reminiscent of the situation where β_2m is part of an MHC class I complex. For example, the interactions include Phe56, Trp60 and Phe62. All of these residues are highly conserved from fish to human (Fig. S2) and may exhibit, despite their involvement in multiple hydrophobic contacts, considerable flexibility (high B-factor) in both polypeptide chains within the asymmetric unit, as in the case of Phe56 and Trp60 (Fig. S3). We also noticed that several residues located in this segment (from D_1 to E strand) are flexible in free β_2m, exhibiting either poorly defined electron density (Phe56) or double conformations (Ser55, Asp58 and also Trp60) (Fig. 4B). In the NMR structure of monomeric human β_2m, an increased conformational flexibility of the same segment was observed [44]. This segment becomes stabilized upon binding of β_2m to an HC, as observed in the structure of chicken β_2m in complex with the HC of YF1*7.1 (Fig. 4C) [19] where the indole moiety of Trp60 adopts a single conformation that intercalates between HC residues which reside on the floor of the peptide binding groove.

3.4. Structural comparison of monomeric β_2m structures

Compared to the vast number of β_2m structures solved as part of MHC class I molecules deposited in the PDB, a structure of free β_2m is only available from four species, namely chicken (PDB entry: 3O81, this study), bovine (1BMG) [1], human (1LDS) [45], and (2YXF) [46] as well as carp (3GBL) [47]. In addition, there is structural information available for the human protein obtained by NMR spectroscopy [44,45,48].

The overall fold of all free β_2m structures is very similar. Superposition of the 97 Cα-atom pairs of chicken and human β_2m results in an r.m.s.d. of 3.5 Å, while chicken and bovine β_2m exhibit an r.m.s.d. of 3.1 Å, and chicken and carp β_2m reveal an r.m.s.d. of 2.6 Å. These relatively small structural differences can be attributed to differences between the β-sandwiches of these proteins (Fig. 6). The most drastic conformational difference between β_2m of other species and their human counterpart, however, is seen in the AB loop (residues 12–20). The AB loop of human β_2m points away from the β-sandwich,

A

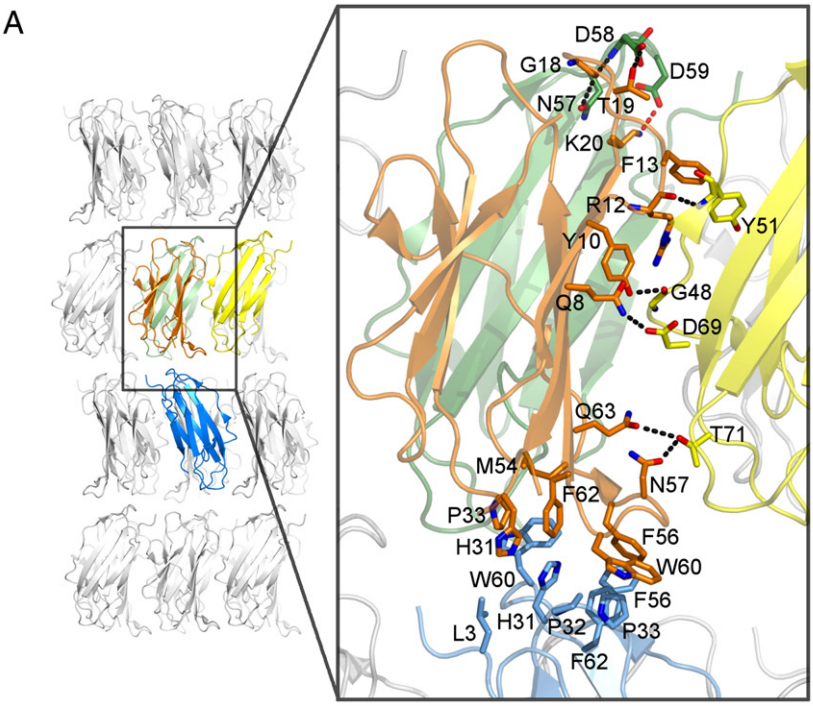

B

		Distance (Å)	Interaction
$Q8^{NE2}$	$D69^{OD2}$	2.77	HB
$Y10^{OH}$	$G48^{O}$	2.71	HB
$R12^{O}$	$Y51^{N}$	2.76	HB
F13	Y51	3.54-3.96	π-stack
$G18^{O}$	$N57^{OD1}$	3.46	HB
$G18^{O}$	$D58^{N}$	2.68	HB
$T19^{OG1}$	$D58^{OD2}$	2.39	HB
$K20^{NZ}$	$D59^{OD2}$	3.51	SB
H31	L3	3.80	vdW
H31	H31	3.31-3.72	vdW
P33	W60	3.42-3.98	vdW
M54	W60	3.49-3.80	vdW
F56	F62	3.95-3.98	vdW
F56	F56	3.32-3.94	vdW
$N57^{OD1}$	$T71^{OG1}$	2.80	HB
W60	P33	3.42-3.98	vdW
W60	F62	3.26-3.99	vdW
F62	W60	3.26-3.99	vdW
$Q63^{OE1}$	$T71^{OG1}$	3.41	HB

Fig. 5. Crystal lattice and interface contacts of chicken β_2m. (A) The two β_2m molecules in the asymmetric unit are colored as orange and blue. The residues involved in the head-to-head arrangement of the two β_2m molecules are exclusively hydrophobic. Further interface contacts are observed with neighboring symmetry-related molecules which are colored as green and yellow. Hydrogen bonds and salt bridges are indicated with black and red dashed lines, respectively. (B) Interface contact details as shown in (A). β_2m residues are color-shaded according to the β_2m molecules in (A). Hydrogen bonds and salt bridges are listed with a distance cut-off of 3.5 Å and hydrophobic contacts with a distance cut-off of 4.0 Å. HB = hydrogen bond, SB = salt bridge and vdW = van der Waals interaction.

while the chicken, bovine and carp AB loops lean onto the β-sandwich (Fig. 6A). A further difference concerns the presence of a β-bulge that is flanked by strands D_1^{50-51} and D_2^{55-56} in the chicken, bovine and carp β_2m structures, but not in human β_2m (Fig. 6A), where a continuous β-strand D is observed [45]. Trinh and colleagues [45] wondered whether this β-strand persists only under the conditions of crystallization and performed ^{1}H-NMR experiments that revealed the presence of the β-bulge in solution, in agreement with earlier NMR studies [44,48]. Crystal packing must thus be regarded as the most likely reason for an induction of the continuous β-strand D in the crystal structure of free human β_2m [49].

The C'^{45-46} β-strand and the downstream C'D1 loop region adopt different conformations in all structures (Fig. 6A). This is most likely due to the low level of sequence conservation in the amino acid sequence of the four β_2m molecules (Supplementary Information).

3.5. Structural comparison of free and complexed β_2m

Superposition of the Cα backbones of free and complexed chicken β_2m in the structures BF2*2101 (PDB entry: 3BEV, 3BEW [20], CD1-1 (3JVG) [21] and YF1*7.1 (3P77) [19]) reveal that the four β_2m structures are very similar, with r.m.s.d. of maximally 0.6 Å (Fig. 6B). The

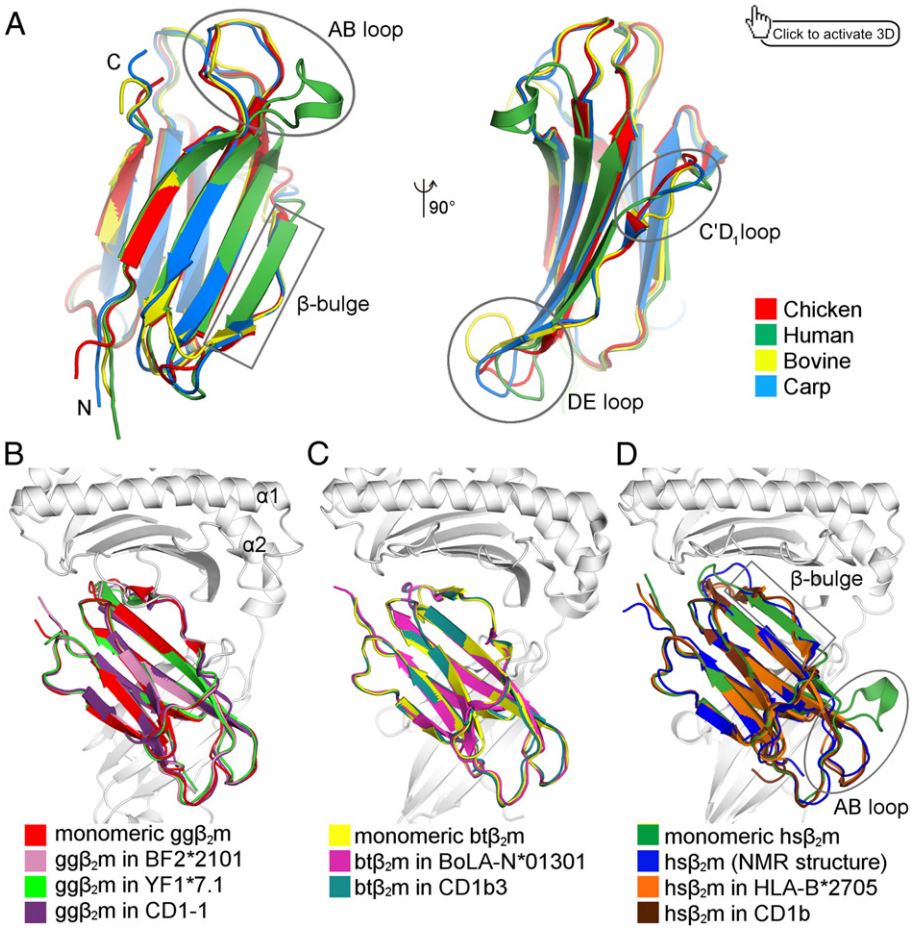

Fig. 6. Comparison of β_2m structures. (A) Overlay of monomeric β_2m structures from chicken, human, bovine and carp. Segments with drastic conformational changes between the molecules are highlighted with grey boxes or ellipses. The human β_2m crystal structure differs considerably from the other β_2m structures in two regions, the AB loop and the absence of a β-bulge between the D_1-D_2 strands. Other significant differences between the β_2m molecules compared here are the C'D_1 and DE loops that may exhibit high flexibility. (B) Overlay of monomeric chicken β_2m (ggβ_2m) and ggβ_2m bound to classical class I BF2*2101 and YF1*7.1 as well as to the non-classical CD1-1 molecule of the chicken. (C) Overlay of monomeric bovine β_2m (btβ_2m) and btβ_2m associated with BoLA-N*01301 and bovine CD1b3. As in the case of the chicken β_2m structures, bovine β_2m is structurally identical, whether in the monomeric or the bound form. (D) Overlay of monomeric human β_2m (hsβ_2m) as observed by X-ray crystallization (green) or NMR spectroscopy (blue), together with hsβ_2m as part of HLA-B*27:05 and human CD1b complexes. Areas bordered with grey lines indicate the drastic difference in the crystal structure of hsβ_2m (green) compared to the other hsβ_2m. For the ease of comparison, a three-dimensional figure is embedded here; see Methods for instructions. PDB entries of structures used to generate the figures are chicken β_2m (3O81), BF2*2101 (3BEW), YF1*7.1 (3P77), CD1-1 (3JVG); human β_2m (1LDS), human β_2m from NMR spectroscopy (1JNJ), HLA-B*27:05 (1OGT), CD1b (2H26); bovine β2m (1BMG), BoLA-N*01301 (2XFX), CD1b3 (3L9R); carp β_2m (3GBL).

largest differences between free and bound β_2m are found at both polypeptide termini due to different contacts between β_2m and HC residues. The structures of free bovine β_2m and this protein in complex with the HC of bovine BoLA-N*01301 (2XFX) [50] or CD1b3 (3L9R) [51] are also nearly identical, with r.m.s.d. of 0.5 Å (Fig. 6C). In contrast, the crystal structure of free human β_2m differs significantly (r.m.s.d. of 3.1 Å) from that of the HC-complexed human protein. For example, the HLA–B*27:05-complexed β_2m (2A83) [52] is distinct at two particular segments: the β-bulge region between the D_1–D_2 strands and the AB loop as described in the previous section. Upon binding to the HC, the two segments of human β_2m "revert" back to the typical conformations seen in the free forms of chicken, bovine and carp β_2m (Fig. 6B, C, D and Supplemental Information). We noticed that residues in the chicken monomeric β_2m exhibit flexibility, such as Asp53, Ser55, Phe56 and Trp60, which are stabilized when associated with the HC of the four complexes referred to previously [19–21].

The comparison provided in Fig. S2 demonstrates that proteins sharing ~48% amino acid sequence similarity (chicken and mammalian β_2m) or even only ~35% similarity (chicken and carp β_2m) can have practically identical structures. It is very likely that a distinct set of highly conserved residues that engage in intra-molecular contacts is responsible for this finding. As hydrophobic intra-chain contacts are too numerous to be listed here, Table S1 provides all such contacts that are due to salt bridges or hydrogen bonds. Four highly conserved contacts are seen in β_2m molecules of all four species (R/H12–N21; N21–F/Y/V/T22; N/D42–D/S76/75; N/D42–E/Q/T76/77; colored yellow Table S1), although different side chain functions can be involved. In addition, there are further contacts that are conserved in three of the four molecules investigated here (colored green in Table S1). We also notice that the number of salt bridges (colored pink in Supplemental Information Table S1) differs between the four proteins. While the chicken polypeptide exhibits only a single salt bridge near its N-terminus, carp β_2m possesses two such contacts, in distinct locations of the molecule. Furthermore, there are three (bovine) or four (human) intra-molecular salt bridges, several of them clustered, in the mammalian proteins. Since thermodynamic analyses have only been carried out on human and chicken β_2m, we cannot be sure whether the relative instability of the avian protein is also a consequence of the distinct endorsement of the two proteins with salt bridges. A unifying feature, however, is the presence and topographical conservation of the S–S bridge which is a hallmark of immunoglobulin domains [53].

In addition, there are more glycine residues in chicken β_2m than in human β_2m (5 versus 3) (Fig. S2). These residues could have an effect on the stability of the former molecule, since glycine residues are able

to contribute to main chain flexibility. Interestingly, one residue (Lys48) involved in intra-molecular salt bridges in human β_2m is substituted by glycine in chicken β_2m (Fig. S2 and Table S1). We have also analyzed the interface complementarity between the two principle sheets of the β_2m molecules, i.e. the ABED and CFG sheets (Fig. 4) as this property might also contribute to the distinct biophysical properties of the chicken and human β_2m. The two β-sheets of chicken β_2m are less complementary than those of human β_2m, with an interface shape complementarity score of 0.69 and 0.65 for the two symmetrical monomers in the crystal lattice in the case of the former protein (PDB entry: 3O81) and 0.75 for the latter molecule (PDB entry 1LDS). Interfaces with a shape complementarity score of "1" will match precisely, while a value of "0" is an indicator for complete lack of complementarity [38].

4. Conclusions

The main interest for embarking on biophysical studies of β_2m is very likely the involvement of the human protein in dialysis-related amyloidosis. We are not aware of β_2m-related amyloidosis in chickens, although other forms of amyloidosis do exist in this species [18]. Our results reveal, however, that despite overall structural conservation, β_2-microglobulins from human and chicken exhibit differential stability and conformational flexibility. Structurally conserved, but thermodynamically and sequence-divergent β_2m molecules might thus be regarded as products of "restrained" evolution, since this monomorphic protein is under the pressure to bind to a vast variety of HC ranging from polymorphic classical MHC class I chains to distantly related MHC class I-like molecules such as CD1. Since biophysical characteristics are expected to impact on the aggregation behavior of a protein, future studies on the aggregation and fibril formation properties of chicken β_2m might provide interesting information on several aspects of protein misfolding.

Acknowledgments

The cDNA was a kind gift of M. M. Miller and R. Goto. We are grateful to M. Wahl for continuous encouragement and support. This work was supported by the Deutsche Forschungsgemeinschaft (grants Na226/12-3, UC8/1-2, and SFB 449/B6). A. Ziegler acknowledges financial support by the Volkswagen Stiftung (grant I/79 989). B. Loll is grateful for support by the Forschungskommission of the Freie Universität Berlin as well as the Fonds der Chemischen Industie. C.-S. Hee was supported by the Berliner Krebsgesellschaft and the Deutsche Forschungsgemeinschaft. We acknowledge access to beamline BL14.2 of the BESSY II storage ring (Berlin, Germany) *via* the Joint Berlin MX-Laboratory sponsored by the Helmholtz Zentrum Berlin für Materialien und Energie, the Freie Universität Berlin, the Humboldt-Universität zu Berlin, the Max-Delbrück Centrum and the Leibniz-Institut für Molekulare Pharmakologie.

Appendix A. Supplementary data

Supplementary data to this article can be found online at http://dx.doi.org/10.1016/j.bpc.2012.04.001.

References

[1] J.W. Becker, G.N. Reeke Jr., Three-dimensional structure of β_2-microglobulin, Proceedings of the National Academy of Sciences of the United States of America 82 (1985) 4225–4229.
[2] T. Hunkapiller, L. Hood, Diversity of the immunoglobulin gene superfamily, Advances in Immunology 44 (1989) 1–63.
[3] M.A. Saper, P.J. Bjorkman, D.C. Wiley, Refined structure of the human histocompatibility antigen HLA-A2 at 2.6 A resolution, Journal of Molecular Biology 219 (1991) 277–319.
[4] Z. Zeng, A.R. Castano, B.W. Segelke, E.A. Stura, P.A. Peterson, I.A. Wilson, Crystal structure of mouse CD1: an MHC-like fold with a large hydrophobic binding groove, Science 277 (1997) 339–345.
[5] G.R. Otten, E. Bikoff, R.K. Ribaudo, S. Kozlowski, D.H. Margulies, R.N. Germain, Peptide and beta 2-microglobulin regulation of cell surface MHC class I conformation and expression, Journal of Immunology 148 (1992) 3723–3732.
[6] D. Lancet, P. Parham, J.L. Strominger, Heavy chain of HLA-A and HLA-B antigens is conformationally labile: a possible role for beta 2-microglobulin, Proceedings of the National Academy of Sciences of the United States of America 76 (1979) 3844–3848.
[7] M.S. Krangel, H.T. Orr, J.L. Strominger, Assembly and maturation of HLA-A and HLA-B antigens in vivo, Cell 18 (1979) 979–991.
[8] M. Fellous, A. Gerbal, G. Nobillot, J. Weils, Studies on the biosynthetic pathway of human P erythrocyte antigen using genetic complementation tests between fibroblasts from rare p and Pk phenotype donors, Vox Sanguinis 32 (1977) 262–268.
[9] B. Dobberstein, S. Kvist, L. Roberts, Structure and biosynthesis of histocompatibility antigens (H-2, HLA), Philosophical Transactions of the Royal Society of London. Series B, Biological Sciences 300 (1982) 161–172.
[10] D.B. Williams, B.H. Barber, R.A. Flavell, H. Allen, Role of Beta-2-microglobulin in the intracellular-transport and surface expression of murine class-I histocompatibility molecules, Journal of Immunology 142 (1989) 2796–2806.
[11] M. Zijlstra, M. Bix, N.E. Simister, J.M. Loring, D.H. Raulet, R. Jaenisch, Beta 2-microglobulin deficient mice lack CD4-8+ cytolytic T cells, Nature 344 (1990) 742–746.
[12] P.A. Peterson, L. Rask, L. Ostberg, beta2-microglobulin and the major histocompatibility complex, Advances in Cancer Research 24 (1977) 115–163.
[13] C. Vincent, J.P. Revillard, B. Charpentier, Presence of glycoproteins binding human beta 2 microglobulin in rat serum, Comptes Rendus des Séances de l'Académie des sciences. Série III 292 (1981) 755–758.
[14] J. Cejka, J.A. Van Nieuwkoo, D.W. Mood, K. Kithier, J. Radl, Beta2-microglobulin in human colostrum and milk: effect of breast feeding and physico-chemical characterization, Clinica Chimica Acta 67 (1976) 71–78.
[15] J.F. Winchester, J.A. Salsberg, N.W. Levin, Beta-2 microglobulin in ESRD: an in-depth review, Advances in Renal Replacement Therapy 10 (2003) 279–309.
[16] N.H. Heegaard, beta(2)-microglobulin: from physiology to amyloidosis, Amyloid 16 (2009) 151–173.
[17] G.W. Platt, S.E. Radford, Glimpses of the molecular mechanisms of beta2-microglobulin fibril formation in vitro: aggregation on a complex energy landscape, FEBS Letters 583 (2009) 2623–2629.
[18] W.J. Landman, Amyloid arthropathy in chickens, Veterinary Quarterly 21 (1999) 78–82.
[19] C.S. Hee, S. Gao, B. Loll, M.M. Miller, B. Uchanska-Ziegler, O. Daumke, A. Ziegler, Structure of a classical MHC Class I molecule that binds "non-classical" ligands, PLoS Biology 8 (2010) e1000557.
[20] M. Koch, S. Camp, T. Collen, D. Avila, J. Salomonsen, H.J. Wallny, A. van Hateren, L. Hunt, J.P. Jacob, F. Johnston, D.A. Marston, I. Shaw, P.R. Dunbar, V. Cerundolo, E.Y. Jones, J. Kaufman, Structures of an MHC class I molecule from B21 chickens illustrate promiscuous peptide binding, Immunity 27 (2007) 885–899.
[21] H. Dvir, J. Wang, N. Ly, C.C. Dascher, D.M. Zajonc, Structural basis for lipid-antigen recognition in avian immunity, Journal of Immunology 184 (2010) 2504–2511.
[22] D.N. Garboczi, D.T. Hung, D.C. Wiley, HLA-A2-peptide complexes—refolding and crystallization of molecules expressed in *Escherichia coli* and complexed with single antigenic peptides, Proceedings of the National Academy of Sciences of the United States of America 89 (1992) 3429–3433.
[23] C.S. Hee, S. Gao, M.M. Miller, R.M. Goto, A. Ziegler, O. Daumke, B. Uchanska-Ziegler, Expression, purification and preliminary X-ray crystallographic analysis of the chicken MHC class I molecule YF1*7.1, Acta Crystallographica. Section F, Structural Biology and Crystallization Communications 65 (2009) 422–425.
[24] M.A. Sherman, R.M. Goto, R.E. Moore, H.D. Hunt, T.D. Lee, M.M. Miller, Mass spectral data for 64 eluted peptides and structural modeling define peptide binding preferences for class I alleles in two chicken MHC-B haplotypes associated with opposite responses to Marek's disease, Immunogenetics 60 (2008) 527–541.
[25] R.C. Hillig, M. Hülsmeyer, W. Saenger, K. Welfle, R. Misselwitz, H. Welfle, C. Kozerski, A. Volz, B. Uchanska-Ziegler, A. Ziegler, Thermodynamic and structural analysis of peptide- and allele-dependent properties of two HLA-B27 subtypes exhibiting differential disease association, Journal of Biological Chemistry 279 (2004) 652–663.
[26] H. Fabian, K. Gast, M. Laue, R. Misselwitz, B. Uchanska-Ziegler, A. Ziegler, D. Naumann, Early stages of misfolding and association of beta2-microglobulin: insights from infrared spectroscopy and dynamic light scattering, Biochemistry 47 (2008) 6895–6906.
[27] W. Kabsch, XDS, Acta Crystallographica. Section D, Biological Crystallography 66 (2010) 125–132.
[28] A.J. McCoy, R.W. Grosse-Kunstleve, P.D. Adams, M.D. Winn, L.C. Storoni, R.J. Read, Phaser crystallographic software, Journal of Applied Crystallography 40 (2007) 658–674.
[29] G.N. Murshudov, A.A. Vagin, A. Lebedev, K.S. Wilson, E.J. Dodson, Efficient anisotropic refinement of macromolecular structures using FFT, Acta Crystallographica. Section D, Biological Crystallography 55 (Pt 1) (1999) 247–255.
[30] P. Emsley, B. Lohkamp, W.G. Scott, K. Cowtan, Features and development of Coot, Acta Crystallographica. Section D, Biological Crystallography 66 (2010) 486–501.
[31] M.D. Winn, M.N. Isupov, G.N. Murshudov, Use of TLS parameters to model anisotropic displacements in macromolecular refinement, Acta Crystallographica. Section D, Biological Crystallography 57 (2001) 122–133.

[32] R.A. Laskowski, M.W. McArthur, D.S. Moss, J.M. Thornton, PROCHECK: a program to check the stereochemical quality of protein structures, Journal of Applied Crystallography 26 (1993) 283–291.
[33] V.B. Chen, W.B. Arendall III, J.J. Headd, D.A. Keedy, R.M. Immormino, G.J. Kapral, L.W. Murray, J.S. Richardson, D.C. Richardson, MolProbity: all-atom structure validation for macromolecular crystallography, Acta Crystallographica. Section D, Biological Crystallography 66 (2010) 12–21.
[34] W. Kabsch, C. Sander, Dictionary of protein secondary structure: pattern recognition of hydrogen-bonded and geometrical features, Biopolymers 22 (1983) 2577–2637.
[35] E. Krissinel, K. Henrick, Secondary-structure matching (SSM), a new tool for fast protein structure alignment in three dimensions, Acta Crystallographica. Section D, Biological Crystallography 60 (2004) 2256–2268.
[36] J. Dundas, Z. Ouyang, J. Tseng, A. Binkowski, Y. Turpaz, J. Liang, CASTp: computed atlas of surface topography of proteins with structural and topographical mapping of functionally annotated residues, Nucleic Acids Research 34 (2006) W116–W118.
[37] W.L. DeLano, The PyMOL Molecular Graphics System on World Wide Web, 2002 http://www.pymol.org.
[38] M.C. Lawrence, P.M. Colman, Shape complementarity at protein/protein interfaces, Journal of Molecular Biology 234 (1993) 946–950.
[39] P. Kumar, A. Ziegler, A. Grahn, C.S. Hee, A. Ziegler, Leaving the structural ivory tower, assisted by interactive 3D PDF, Trends in Biochemical Sciences 35 (2010) 419–422.
[40] S.W. Englander, N.R. Kallenbach, Hydrogen exchange and structural dynamics of proteins and nucleic acids, Quarterly Reviews of Biophysics 16 (1983) 521–655.
[41] R. Bolzani, F. Ruggeri, O.M. Olivo, Average normal temperature of the chicken in the morning and after 1–2 days of fasting, Bollettino della Società Italiana di Biologia Sperimentale 55 (1979) 1618–1622.
[42] H.J. Wallny, D. Avila, L.G. Hunt, T.J. Powell, P. Riegert, J. Salomonsen, K. Skjodt, O. Vainio, F. Vilbois, M.V. Wiles, J. Kaufman, Peptide motifs of the single dominantly expressed class I molecule explain the striking MHC-determined response to Rous sarcoma virus in chickens, Proceedings of the National Academy of Sciences of the United States of America 103 (2006) 1434–1439.
[43] A. Ziegler, B. Loll, R. Misselwitz, B. Uchanska-Ziegler, Implications of structural and thermodynamic studies of HLA-B27 subtypes exhibiting differential association with ankylosing spondylitis, Advances in Experimental Medicine and Biology 649 (2009) 177–195.
[44] G. Verdone, A. Corazza, P. Viglino, F. Pettirossi, S. Giorgetti, P. Mangione, A. Andreola, M. Stoppini, V. Bellotti, G. Esposito, The solution structure of human β2-microglobulin reveals the prodromes of its amyloid transition, Protein Science 11 (2002) 487–499.
[45] C.H. Trinh, D.P. Smith, A.P. Kalverda, S.E. Phillips, S.E. Radford, Crystal structure of monomeric human β-2-microglobulin reveals clues to its amyloidogenic properties, Proceedings of the National Academy of Sciences of the United States of America 99 (2002) 9771–9776.
[46] K. Iwata, T. Matsuura, K. Sakurai, A. Nakagawa, Y. Goto, High-resolution crystal structure of β_2-microglobulin formed at pH 7.0, Journal of Biochemistry 142 (2007) 413–419.
[47] W. Chen, F. Gao, F. Chu, J. Zhang, G.F. Gao, C. Xia, Crystal structure of a bony fish β_2-microglobulin: insights into the evolutionary origin of immunoglobulin superfamily constant molecules, Journal of Biological Chemistry 285 (2010) 22505–22512.
[48] M. Okon, P. Bray, D. Vucelic, ^{1}H NMR assignments and secondary structure of human β2-microglobulin in solution, Biochemistry 31 (1992) 8906–8915.
[49] S. Ricagno, S. Raimondi, S. Giorgetti, V. Bellotti, M. Bolognesi, Human beta-2 microglobulin W60V mutant structure: implications for stability and amyloid aggregation, Biochemical and Biophysical Research Communications 380 (2009) 543–547.
[50] I.K. Macdonald, M. Harkiolaki, L. Hunt, T. Connelley, A.V. Carroll, N.D. MacHugh, S.P. Graham, E.Y. Jones, W.I. Morrison, D.R. Flower, S.A. Ellis, MHC class I bound to an immunodominant Theileria parva epitope demonstrates unconventional presentation to T cell receptors, PLoS Pathogens 6 (2010) e1001149.
[51] E. Girardi, J. Wang, T.T. Mac, C. Versluis, V. Bhowruth, G. Besra, A.J. Heck, I. Van Rhijn, D.M. Zajonc, Crystal structure of bovine CD1b3 with endogenously bound ligands, Journal of Immunology 185 (2010) 376–386.
[52] C. Rückert, M.T. Fiorillo, B. Loll, R. Moretti, J. Biesiadka, W. Saenger, A. Ziegler, R. Sorrentino, B. Uchanska-Ziegler, Conformational dimorphism of self-peptides and molecular mimicry in a disease-associated HLA-B27 subtype, Journal of Biological Chemistry 281 (2006) 2306–2316.
[53] P.J. Bjorkman, M.A. Saper, B. Samraoui, W.S. Bennett, J.L. Strominger, D.C. Wiley, Structure of the human class I histocompatibility antigen, HLA-A2, Nature 329 (1987) 506–512.